Spectra of Digital FM

By R. R. ANDERSON and J. SALZ

(Manuscript received March 29, 1965)

Formulas are derived for the spectral density function of an ensemble of continuous-phase, constant-envelope FM waves. The modulation signals are random time series of the form $\sum_n a_n g(t - nT)$, *where* $g(t)$ *is an arbitrary pulse of finite duration* rT, $r \geqq 1$. *The* a_n*'s are independent random variables possessing identical but otherwise arbitrary probability distribution. The derived results are general and are presented in terms of averages of elementary functions. When the* a_n*'s are discrete random variables, both continuous and discrete spectra are treated, and conditions in terms of the modulation parameters are given under which discrete spectral lines are present. Several of our specialized formulas are applicable in the study of multilevel FM data transmission systems as well as in pulse frequency modulation.*

I. INTRODUCTION

Progress in analysis of multilevel frequency shift keying (FSK) has lagged behind that of binary. Inherent difficulties associated with an increase in the number of levels are partly responsible, but activity also has been inhibited by the general impression that multilevel FSK is inferior to differential phase modulation with the same number of levels operating in the same bandwidths.

Recent work, Ref. 1, has evolved design principles showing a possibility of substantial improvements in multilevel FM performance over that formerly thought to be typical. Also there are many existing analog channels, e.g., in microwave radio relay, which operate by FM. Attempts to send digital data efficiently over such channels force consideration of the multilevel FSK problem.

An important item in the statistical description of an information-bearing signal is the spectral density, which defines the average power density of the signal as a function of frequency. In addition to furnishing an estimate of bandwidth requirements, the spectral density is critically important in optimization procedures for minimizing the effect of channel noise subject to a constraint on mean total transmitting signal power. Evaluation of mutual interference between channels also requires knowledge of spectral distribution.

From the practical point of view the most interesting case of digital FM is that in which the phase is continuous at the transitions, as may be obtained at the output of a keyed oscillator. The memory thus introduced makes the analysis far from trivial. So far as is known, the binary case is the only continuous-phase FSK problem hitherto covered in the literature. The present paper gives a complete analytic solution for a general set of parameters.

An interesting feature is the extent to which sharp spectral peaks occur near the discrete signaling frequencies. These peaks can, under certain conditions, become delta functions indicating steady sine-wave components. Such components make the design of optimum filters difficult because the best results usually demand sharply tuned suppression of the corresponding regions at the transmitter and complementary high gain peaks at the receiver. Furthermore, the interference produced in other channels by untreated peaked spectra can be inordinately severe. One important result of the analysis is an establishment of conditions on the frequency spacing relative to signaling rate such that spectral peaking does not occur.

In this paper we derive compact formulas for the spectral density function of an ensemble of continuous-phase, constant-envelope FM waves. The frequency of the wave is switched every T seconds by a known signal. The phase of the wave is so adjusted as to maintain continuity at the transitions. For example, when the baseband signal is a rectangular pulse of T seconds in duration, the frequency of the wave during each interval T may be one out of many different frequencies picked at random. In general, the baseband signal is not time limited to T seconds. This case will arise when the original time limited signal is passed through a filter.

The random signal whose spectral density we wish to study has the following standard representation:

$$S(t) = A \cos \left\{ \omega_c t + \omega_d \sum_{n=0}^{n=\infty} a_n \int_0^t g(t' - nT)\, dt' + \varphi \right\} \qquad (1)$$

$$0 \leqq t \leqq \infty$$

where ω_c and ω_d are arbitrary angular frequencies. The angle φ is a uniformly distributed random variable (r.v.) on $[0,2\pi]$ and the a_n's are independent r.v.'s with arbitrary but identical probability distribution. The symbol A is an arbitrary real amplitude.

The only restriction on the baseband signal $g(t)$ is that

$$g(t) = \begin{cases} g_r(t), & 0 \leqq t \leqq rT \\ 0, & \text{everywhere else} \end{cases} \tag{2}$$

where r is an arbitrary positive integer. (We naturally require that $g(t)$ be integrable over this interval.) When the a_n's are binary r.v.'s and $g(t)$ is a rectangular pulse of T seconds duration, spectra and correlation functions have recently been derived by Bennett and Rice, Ref. 2. Salz, Ref. 3, extended Bennett's and Rice's results to include arbitrary a_n's possessing arbitrary probability distributions.

In our treatment the distribution of the a_n's as well as $g(t)$ is entirely arbitrary. For instance when $g(t)$ is a rectangular pulse and the a_n's are discrete r.v.'s, the wave (1) represents the ensemble of multilevel FM waves. If the a_n's correspond to the samples of speech taken every T seconds, we have pulse amplitude modulation via frequency shift keying. Many other applications depending on the choice of the a_n's and $g(t)$ may be cited, and are covered in our results.

Our method of attack on the problem is direct. We calculate the segmented Fourier transform of (1), obtain its magnitude squared, average over all random variables, divide by the length of the segment, and then evaluate the limit as the length increases without bound. After considerable amount of bookkeeping, we obtain general formulas. We then specialize the formulas, and investigate some interesting representative cases. The general formula for the continuous spectrum is given in (31). Equation (40) is the general formula for the discrete as well as the continuous spectrum.

II. GENERAL DEVELOPMENT

We found it easier to work with the complex representation of (1). Therefore let

$$S(t) = \frac{A}{2}\,[z(t) + z^*(t)] \qquad 0 \leqq t \leqq \infty \tag{3}$$

where

$$z(t) = e^{i\varphi} \exp i\left\{\omega_c t + \omega_d \sum_{n=0}^{n=\infty} a_n \int_{-nT}^{t-nT} g(t')\,dt'\right\}. \tag{4}$$

The symbol * denotes the complex conjugation.

Choose a finite interval $[0,NT]$. Over this interval the Fourier transform of $z(t)$ is

$$
\begin{aligned}
Z(\omega,NT) &= \sum_{k=0}^{k=N-1} \int_{kT}^{(k+1)T} z(t)e^{-\omega t}dt \\
&= e^{i\varphi} \sum_{k=0}^{k=N-1} Q_k
\end{aligned}
\tag{5}
$$

where

$$
Q_k = \int_{kT}^{(k+1)T} dt \exp i(\omega_c - \omega)t \prod_{n=0}^{n=\infty} \exp i\left\{\omega_d a_n \int_{-nT}^{t-nT} g(t')dt'\right\}. \tag{6}
$$

Set $t - kT = y$ above to obtain

$$
Q_k = e^{ikT(\omega_c-\omega)} \int_0^T dy \exp i(\omega_c - \omega)y \prod_{n=0}^{n=\infty} P_{n,k}(y) \tag{7}
$$

where

$$
P_{n,k}(y) = \exp i\left\{\omega_d a_n \int_{-nT}^{y-(n-k)T} g(t')dt'\right\}. \tag{8}
$$

Since $g(t)$ is time limited to rT, where r is a positive integer, it follows that we can write $P_{n,k}(y)$ for $0 \leqq y \leqq T$, as;

$$
P_{n,k}(y) = \begin{cases}
\exp\left[i\omega_d a_n \int_0^{rT} g_r(t')dt'\right], & 0 \leqq n \leqq k - r \\
\exp\left[i\omega_d a_n \int_0^{y-(n-k)T} g(t')dt'\right], & k - r + 1 \leqq n \leqq k \\
1 & n > k.
\end{cases}
\tag{9}
$$

With this representation, we can take the product in (7) running from $n = 0$ to $n = k - r$ outside the integral sign since $P_{n,k}(y)$ in this range of n does not depend on y. $P_{n,k}(y)$ depends on y only in the range $k - r + 1 \leqq n \leqq k$. Making use of these facts, we write for Q_k

$$
Q_k = e^{ikT\nu} \exp i\left\{\alpha_r \sum_{n=0}^{n=k-r} a_n\right\} F(\nu,a_{k-r+1} \cdots a_k) \tag{10}
$$

where

$$
\begin{aligned}
F(\nu,a_{k-r+1} \cdots a_k) \\
&= \int_0^T e^{i\nu y} \prod_{n=k-r+1}^{n=k} \exp i\left\{\omega_d a_n \int_0^{y-(n-k)T} g_r(t')dt'\right\} dy \\
&= \int_0^T e^{i\nu y} \exp i\left\{\sum_{m=1}^{m=r} a_{k-r+m} V[y - (m - r)T]\right\} dy,
\end{aligned}
\tag{11}
$$

and

$$\begin{aligned} \alpha_r &= \omega_d \int_0^{rT} g_r(t)\,dt \\ \nu &= \omega_c - \omega \\ V(\xi) &= \omega_d \int_0^{\xi} g(t)\,dt. \end{aligned} \tag{12}$$

The segmented Fourier transform of the original signal (3) is

$$\begin{aligned} S(\omega,NT) &= \frac{A}{2}\,[Z(\omega,NT) + Z_c(\omega,NT)] \\ &= \frac{A}{2}\left[e^{i\varphi} \sum_{k=0}^{k=N-1} Q_k + e^{-i\varphi} \sum_{k=0}^{k=N-1} Q_{ck}\right] \end{aligned} \tag{13}$$

where $Z_c(\omega,NT)$ is the Fourier Transform of $Z^*(\omega,N)$ given as

$$\begin{aligned} Z_c(\omega,NT) &= \sum_{k=0}^{k=N-1} \int_{kT}^{(k+1)T} z^*(t)\,e^{-i\omega t}\,dt \\ &= Ae^{-i\varphi} \sum_{k=0}^{k=N-1} Q_{ck}\,, \end{aligned} \tag{14}$$

and

$$\begin{aligned} Q_{ck} = \int_{kT}^{(k+1)T} dt \exp -i(\omega_c + \omega)t \\ \cdot \prod_{n=0}^{n=\infty} \exp -i\left\{\omega_d a_n \int_{-nT}^{t-nT} g(t')\,dt'\right\}. \end{aligned} \tag{15}$$

The magnitude squared of $S(\omega,NT)$ averaged with respect to the r.v. φ is

$$\langle |S(\omega,NT)|^2\rangle_\varphi = \frac{A^2}{4}\left[\sum_{k,s=0}^{k,s=N-1} Q_k Q_s{}^* + \sum_{k,s=0}^{k,s=N-1} Q_{cs} Q_{ck}{}^*\right]. \tag{16}$$

The symbol $\langle\cdot\rangle$ denotes the averaging operator.

From the definition of Q_k in (10) we obtain

$$\begin{aligned} Q_k Q_s{}^* = e^{iT\nu(k-s)} F(\nu,a_{k-r+1} \cdots a_k) F^*(\nu,a_{s-r+1} \cdots a_s) \\ \cdot \exp i\left\{\alpha_r\left[\sum_{n=0}^{n=k-r} a_n - \sum_{n=0}^{n=s-r} a_n\right]\right\}. \end{aligned} \tag{17}$$

We observe that $Q_{cs}Q_{ck}{}^*$ equals $Q_kQ_s{}^*$ with $\omega_c - \omega$ replaced by $\omega_c + \omega$.

It is thus sufficient to continue our calculation using only the first sum in (16).

If we let the first term in (16) be $W_+(\omega)$ and the second term $W_-(\omega)$, the desired power spectrum $G(\omega)$ is by definition

$$G(\omega) = \lim_{N\to\infty} (2/TN)\{\langle W_+(\omega)\rangle_{\mathbf{a}} + \langle W_-(\omega)\rangle_{\mathbf{a}}\} \tag{18}$$

where the ensemble average is taken over the collection of r.v.'s $\mathbf{a} = (a_0, a_1 \cdots a_N)$.

We now proceed to calculate the respective averages. From (16)

$$\begin{aligned} \langle W_+(\omega)\rangle_{\mathbf{a}} &= \frac{A^2}{4} \sum_{k,s=0}^{k,s=N-1} \langle Q_k Q_s^*\rangle_{\mathbf{a}} \\ &= \frac{A^2}{2} \operatorname{Re}\Bigg[\sum_{\substack{k,s \\ \{k<s\}}} \langle Q_k Q_s^*\rangle_{\mathbf{a}} \Bigg] \\ &\quad + \frac{A^2}{4} \sum_{k=0}^{k=N-1} \langle | Q_k |^2\rangle_{\mathbf{a}}. \end{aligned} \tag{19}$$

The symbol "Re[·]" denotes the real part.

To facilitate the evaluation of the averages, we rearrange the double sums above in the following manner:

$$\begin{aligned} \sum_{\substack{k,s=0 \\ \{k>s\}}}^{k,s=N-1} \langle Q_k Q_s^*\rangle_{\mathbf{a}} &= \sum_{s=0}^{s=N-2} \sum_{k=s+1}^{k=N-1} \langle Q_k Q_s^*\rangle_{\mathbf{a}} \\ &= \sum_{s=0}^{s=N-2} \Bigg\{ \langle Q_{s+1} Q_s^*\rangle_{\mathbf{a}} + \langle Q_{s+2} Q_s^*\rangle_{\mathbf{a}} \\ &\qquad + \cdots + \langle Q_{s+r} Q_s^*\rangle_{\mathbf{a}} + \sum_{k=s+r+1}^{k=N-1} \langle Q_k Q_s^*\rangle_{\mathbf{a}} \Bigg\} \\ &= \sum_{s=0}^{s=N-2} \langle Q_{s+1} Q_s^*\rangle_{\mathbf{a}} + \sum_{s=0}^{s=N-3} \langle Q_{s+2} Q_s^*\rangle_{\mathbf{a}} \\ &\qquad + \cdots + \sum_{s=0}^{s=N-r-1} \langle Q_{s+r} Q_s^*\rangle_{\mathbf{a}} \\ &\qquad + \sum_{s=0}^{s=N-r-2} \sum_{k=s+r+1}^{k=N-1} \langle Q_k Q_s^*\rangle_{\mathbf{a}}. \end{aligned} \tag{20}$$

Using the explicit representation of F and F^* in 11, we obtain from 17

$$\begin{aligned}\langle Q_{s+j}Q_s^*\rangle_{\mathbf{a}} &= f_{jr}(\nu), \qquad 1 \leqq j \leqq r \\ &= e^{iT\nu j}\langle F(\nu, a_{s+j-r+1} \cdots a_{s+j}) \\ &\quad \cdot F^*(\nu, a_{s-r+1} \cdots a_s) \exp i\left\{a_r \sum_{n=s-r+1}^{n=s-r+j} a_n\right\}\rangle_{\mathbf{a}} \\ &= e^{iT\nu j}\int_0^T\int_0^T dydy' e^{i\nu(y-y')} \\ &\quad \cdot \langle \exp i\left\{\sum_{m=1}^{m=r} a_{s+j-r+m}V[y-(m-r)T]\right. \\ &\quad \left.-\left\{\sum_{m=1}^{m=r} a_{s-r+m}V[y'-(m-r)T] + a_r\sum_{n=1}^{n=j} a_{s-r+n}\right\}\right\}\rangle_{\mathbf{a}}\end{aligned} \tag{21}$$

Using elementry manipulations we obtain

$$\begin{aligned}f_{jr}(\nu) = e^{iT\nu j}\int_0^T\int_0^T dydy'e^{i\nu(y-y')}\prod_{m=1}^{m=r-j} C_a\{V[y-(m-r)T] \\ -[y'-(m-r+j)T]\}\end{aligned} \tag{22}$$

$$\cdot \prod_{m=1+r-j}^{m=r} C\{V[y-(m-r)T]\}\prod_{m=1}^{m=j} C^*\{V[y'-(m-r)T]-\alpha_r\}.$$

The function

$$C_a(s) = \langle e^{ias}\rangle_a = \int e^{ias}dF(a) \tag{23}$$

is the characteristic function of the r.v. a, and $F(a)$ its probability distribution.

We next calculate in the same manner as above

$$\begin{aligned}\langle Q_kQ_s^*\rangle_a &= e^{iT\nu(k-s)}\left\langle F(\nu, a_{k-r+1} \cdots a_k)F^*(\nu, a_{s-r+1} \cdots a_s)\right. \\ &\quad \left.\cdot \exp i\left\{\alpha_r \sum_{n=s-r+1}^{n=k-r} a_n\right\}\right\rangle_{\mathbf{a}} \\ &= e^{iT\nu(k-s)}\langle F(\nu, a_{k-r+1} \cdots a_k)\rangle_{\mathbf{a}}\left\langle F^*(\nu, a_{s-r+1} \cdots a_s)\right. \\ &\quad \left.\cdot \exp i\left\{\alpha_r \sum_{n=s-r+1}^{n=s} a_n\right\}\right\rangle_{\mathbf{a}} C_a^{k-s-r}(\alpha_r)\end{aligned} \tag{24}$$

when

$$k > s + r.$$

When $k = s$ we have

$$\langle | Q_k |^2 \rangle_{\mathbf{a}} = \langle | F(\nu, a_{k-r+1} \cdots a_k) |^2 \rangle_{\mathbf{a}} . \tag{25}$$

From the definition of F or F^* in (11) we obtain explicitly

$$\begin{aligned} \langle | F(\nu, a_{k-r+1} \cdots a_k) |^2 \rangle_{\mathbf{a}} &= \int_0^T \int_0^T dy dy' e^{i\nu(y-y')} \\ &\cdot \prod_{m=1}^{m=r} C_a \{ V[y - (m - r) T] - V[y' - (m - r) T] \}, \end{aligned} \tag{26}$$

$$\langle F(\nu, a_{k-r+1} \cdots a_k) \rangle_{\mathbf{a}} = \int_0^T e^{i\nu y} \prod_{m=1}^{m=r} C_a \{ V[y - (m - r) T] \} dy \tag{27}$$

and

$$\begin{aligned} &\langle F^*(\nu, a_{s-r+1} \cdots a_s) \exp i \left\{ \alpha_r \sum_{n=s-r+1}^{n=s} a_n \right\} \rangle_{\mathbf{a}} \\ &\qquad = \int_0^T e^{-i\nu y} \prod_{m=1}^{m=r} C_a^* \{ V[y - (m - r) T] - \alpha_r \} dy. \end{aligned} \tag{28}$$

We now observe that the various averages in (22)–(25) are independent of the indices k and s and therefore when we divide (19) or (20) by N and take the limit as N approaches infinity we obtain

$$\begin{aligned} \lim_{N \to \infty} \frac{1}{N} \langle W_+(\omega) \rangle_{\mathbf{a}} &= \frac{A^2}{4} \langle | F(\mathbf{a}) |^2 \rangle_{\mathbf{a}} + \frac{A^2}{2} \operatorname{Re} \left\{ \sum_{j=1}^{j=r} f_{jr}(\nu) \right. \\ &\quad + \langle F_k(\mathbf{a}) \rangle_{\mathbf{a}} \langle F_s(\mathbf{a}) \exp i \left\{ \alpha_r \sum_{n=s-r+1}^{n=s} a_n \right\} \rangle_{\mathbf{a}} \\ &\quad \left. \cdot \lim_{N \to \infty} \frac{1}{N} \sum_{s=0}^{s=N-r-2} \sum_{k=s+r+1}^{k=N-1} e^{iT\nu(k-s)} C_a^{k-s-r}(\alpha_r) \right\} \end{aligned} \tag{29}$$

where we set $F_k(\mathbf{a}) = F(\nu, a_{k-r+1} \cdots a_k)$; $f_{jr}(\nu)$ is defined in (22).

The limit in (26) can readily be evaluated provided $| C_a(\alpha_r) | < 1$. This is the case when we have only continuous spectra. When $| C_a(\alpha_r) | = 1$, the evaluation of the limit is more involved. But this latter is precisely the case when discrete spectra appear, which we shall study in a forthcoming section. For the moment we proceed to evaluate the limit when the modulus of the characteristic function evaluated at α_r is less than unity.

In this case, from (29) we obtain

$$\lim_{N\to\infty} \frac{1}{N} \sum_{s=0}^{s=N-r-2} \sum_{k=s+r+1}^{k=N-1} e^{iT\nu(k-s)} C_a^{k-s-r}(\alpha_r)$$

$$= e^{iT\nu r} \lim_{N\to\infty} \sum_{l=1}^{l=N-r-1} [C_a(\alpha_r) \exp(iT\nu)]^l \quad (30)$$

$$= \frac{e^{iT\nu(r+1)} C_a(\alpha_r)}{1 - e^{iT\nu} C_a(\alpha_r)}.$$

Using the definition of the spectrum in (18) and applying the explicit representation of the averages computed in (22)–(30), we obtain finally the positive image spectrum

$$\begin{aligned} G_+(\nu) = {} & \frac{A^2}{2T} \int_0^T \int_0^T dy dy' e^{i\nu(y-y')} \\ & \cdot \prod_{m=1}^{m=r} C_a\{V[y - (m - r)T] - V[y' - (m - r)T]\} \\ & + \frac{A^2}{T} \operatorname{Re} \left\{ \sum_{j=1}^{j=r} (\text{Equation } 22) \right. \\ & + \frac{e^{iT\nu(r+1)} C_a(\alpha_r)}{1 - e^{iT\nu} C_a(\alpha_r)} \int_0^T dy e^{i\nu y} \\ & \cdot \prod_{m=1}^{m=r} C_a\{V[y - (m - r)T]\} \int_0^T dy e^{-i\nu y} \\ & \left. \cdot \prod_{m=1}^{m=r} C_a^*\{V[y - (m - r)T] - \alpha_r\} \right\}. \end{aligned} \quad (31)$$

Although the final formula may appear rather complicated at first, under close scrutiny it will be observed that the formula is in a convenient form for numerical calculation by a digital computer. At most a double integral on a finite dimensional plane needs to be evaluated. We will later demonstrate, by using a few interesting examples, how the numerical work can be carried out, and the results will be exhibited graphically.

III. SINGULAR CASES

So far we have considered only continuous spectra. In order to arrive at the result of (31) we had to sum the series in (30), and that series converges only when the magnitude of the characteristic function evaluated at α_r is less than unity. This turns out to be the requirement for the spectrum to contain no lines.

Whenever the magnitude of the characteristic function, evaluated at $\alpha_r \neq 0$, is unity we are no longer justified in using the results in (30) since the series diverges. This behavior suggests the presence of discrete spectral lines associated with periodicities in the original random process. Mathematically, this result can only occur if the r.v.'s **a** are discrete and have a definite relationship. The characteristic function of a continuous r.v. must satisfy $| C_a(s)| < | C_a(0)|$ when $s \neq 0$. We proceed to identify the conditions on the a_n which give rise to a characteristic function with unit modulus and therefore spectral lines.

Loève, Ref. 4, shows that if $| C_a(s)| = 1$ for $s \neq 0$, the form of $C_a(s)$ must be

$$C_a(s) = \sum_{k=0}^{k=\infty} P_{a_k} \exp\ (isa_k) \tag{32}$$

where $P_{a_k} \geqq 0$, $\sum_{k=0}^{k=\infty} P_{a_k} = 1$ and the random variables a_k must satisfy

$$a_k = (2\pi/s)k + b \tag{33}$$

where b is an arbitrary constant.

Thus if $| C_a(\alpha_r)| = 1$ the r.v.'s must be integral multiples of one another plus an arbitrary constant common to each of them.

Using (33) in (32) we see that the characteristic function becomes $\exp\ (ibs)$. We set $C_a = \exp\ (ibs)$ and evaluate the following limit:

$$\begin{aligned} \Lambda &= e^{iT\nu r} \lim_{N\to\infty} \frac{1}{N} \sum_{s=0}^{s=N-r-2} \sum_{k=s+r+1}^{k=N-1} e^{-i\gamma(k-s-r)} \\ &= e^{-iT\nu r} \lim_{N\to\infty} \left\{ \sum_{l=1}^{l=N} e^{i\gamma l} + \frac{1}{N} \sum_{l=1}^{l=N} (l + r) e^{i\gamma l} \right\} \end{aligned} \tag{34}$$

where

$$\gamma = T\nu + b\alpha_r .$$

Let

$$\begin{aligned} \Lambda_1(A) &= \sum_{l=1}^{l=\infty} [A \exp i\gamma]^l = \frac{A \exp i\gamma}{1 - A \exp i\gamma} \\ &= i \frac{d}{d\gamma} \ln\ (1 - A \exp i\gamma), \qquad A < 1. \end{aligned} \tag{35}$$

The limit of Λ_1 as $A \to 1$ is the first sum in (34). Obviously this limit does not exist in the ordinary sense. However the "distribution" limit, denoted by $\lim^{(D)}$, Ref. 5, does exist. Barnard, Ref. 6, has shown that

$$\lim_{A\to 1^-}{}^{(D)} \ln (1 - A \exp i\gamma) = \ln |\sin (\gamma/2)| + \ln 2 + i[(\gamma/2) - \pi R_{2\pi}(\gamma) - 2\pi M] \tag{36}$$

where M is an arbitrary integer, and

$$R_{2\pi}(\gamma) = \sum_{n=0}^{\infty} \mu(\gamma - 2\pi n) - \sum_{n=1}^{\infty} \mu(-\gamma - 2\pi n)$$

$$R_{\pi}(\gamma) = R_{2\pi}(\gamma - \pi)$$

$$u(\gamma) = \begin{cases} 1, & \gamma \geqq 0 \\ 0, & \gamma < 0. \end{cases}$$

He also proved that the right side of (36) constitutes a properly defined generalized function or a distribution.

When (36) is differentiated with respect to γ we obtain

$$i \frac{d}{d\gamma} \left\{ \lim_{A\to 1^-} \ln (1 - A \exp i\gamma) \right\} = \frac{i}{2} \cot \frac{\gamma}{2} - \frac{1}{2} + \pi \sum_n \delta(\gamma - 2\pi n) \tag{37}$$

where $\delta(\cdot)$ is the well known dirac delta-function.

The limit of the right hand sum in (34) approaches zero since this sum is proportional to the derivative of the first sum divided by N. Since the first sum is a generalized function or a distribution so is its derivative. Consequently in the distribution sense the limit is zero.

When the characteristic function is of the form (32), which implies that the r.v.'s satisfy (33), we observe that

$$C_a\{V[y + pT] - \alpha_r\} = e^{-ib\alpha_r} C_a\{V[y + pT]\} \tag{38}$$

$$, \qquad p = r - m.$$

From this we obtain

$$\prod_{m=1}^{m=j} C_a^*\{V[y + pT] - \alpha_r\} = e^{b\alpha_r j} \prod_{m=1}^{m=j} C^*[y + pT] \tag{39}$$

Applying (38), (39) in (31), and replacing

$$\frac{e^{iT\nu} C_a(\alpha_r)}{1 - e^{iT\nu} C_a(\alpha_r)}$$

by (37), we obtain for the continuous as well as the discrete spectral density

$$
\begin{aligned}
G_+(\nu) = \frac{A^2}{2T} \int_0^T \int_0^T & dy dy' e^{i\nu(y-y')} \\
& \cdot \prod_{p=0}^{p=r-1} C_a\{V[y + pT] - V[y' + pT]\} \\
& + \frac{A^2}{T} \operatorname{Re} \left\{ \left| \int_0^T dy e^{i\nu y} \prod_{p=0}^{p=r-1} C_a\{V[y + pT]\} \right|^2 \right. \\
& \cdot \left[1 + e^{i\gamma r} \left(\pi \sum_n \delta(\gamma - 2\pi n) - \frac{1}{2} + \frac{i}{2} \cot \frac{\gamma}{2} \right) \right] \\
& \left. + \sum_{j=1}^{j=2-1} f_{jr}(v) \right\}.
\end{aligned} \tag{40}
$$

By recalling the definition of γ in (34) we see that spectral lines occur when

$$T\nu + b\alpha_r = 2\pi n, \tag{41}$$

or

$$\nu = (2\pi n/T) - b(\alpha_r/T)$$

and the minimum spacing $\Delta\nu$ between the lines are given by

$$\Delta\nu = 2\pi\Delta f = \frac{2\pi(n+1)}{T} - \frac{2\pi n}{T} = \frac{1}{T}.$$

IV. SPECIAL CASES

In this section we select several special cases, believed to be of general interest, and exhibit them graphically.

The first case we want to explore is that in which $g(t)$ is a rectangular pulse of unit height and the a_n's are discrete, that is, a frequency shift keying system. For the binary case, the two frequencies are referred to as mark and space frequency, and each is located ω_d from the carrier, ω_c. For the multilevel case the frequency spacing is uniform. In reference to our general formula (31), the following parameters apply:

$$
\begin{aligned}
& r = 1 \\
& V(\xi) = \omega_d \xi, \qquad \alpha_1 = \omega_d T.
\end{aligned} \tag{42}
$$

When (42) is applied in (31) and after considerable manipulation we obtain the specialized formula for the one sided continuous density

$$G(\omega) = \frac{2A^2}{T}\Bigg\{\langle |F(\omega - \omega_c - a\omega_d|^2\rangle_a + 2\,\mathrm{Re}\left[\frac{\exp(iT(\omega_c - \omega))\langle F(\omega - \omega_c - \omega_d)\rangle_a}{1 - C_a(\omega_d T)\exp(iT(\omega_c - \omega))} \cdot \langle F^*(\omega - \omega_c - a\omega_d)\exp(i\omega_d aT)\rangle_a\right]\Bigg\}, \tag{43}$$

where

$$F(\omega) = \frac{T}{2}\exp(-i\omega T/2)\frac{\sin \omega T/2}{\omega T/2}, \tag{44}$$

and

$$|C_a(\omega_d T)| < 1.$$

Let

$$\begin{aligned} \beta &= (\omega - \omega_c)T/2\pi \\ \gamma &= (\omega - \omega_c - a\omega_d)T/2, \end{aligned} \tag{45}$$

and write (43) as

$$G(\beta) = \frac{2A^2}{T}\left\{\left\langle\left|\frac{T}{2}e^{-i\gamma}\frac{\sin\gamma}{\gamma}\right|^2\right\rangle_a + 2\,\mathrm{Re}\left[\frac{e^{-2\pi\beta}\left\langle\frac{T}{2}e^{-i\gamma}\frac{\sin\gamma}{\gamma}\right\rangle_a\left\langle\frac{T}{2}e^{i\gamma}\frac{\sin\gamma}{\gamma}e^{ik\pi a}\right\rangle_a}{1 - e^{-i2\pi\beta}C_a(\omega_d T)}\right]\right\}.$$

$$\frac{G(\beta)}{A^2T} = \frac{I_1}{2} + \mathrm{Re}\left[\frac{I_2^2}{1 - C_a(\omega_d T)e^{-i2\pi\beta}}\right] \tag{46}$$

where

$$\begin{aligned} I_1 &= \left\langle\frac{\sin^2\gamma}{\gamma^2}\right\rangle_a \\ I_2 &= \left\langle\frac{\sin\gamma}{\gamma}e^{-i\gamma}\right\rangle_a. \end{aligned} \tag{47}$$

For binary frequency shift keying, the frequency deviation parameter, k, may be defined as the ratio of frequency shift (the difference between mark and space frequency) to the signaling frequency (the sum of the number of marks and the number of spaces in one second). That is,

$$k = \frac{\omega_m - \omega_s}{2\pi/T} = \frac{\omega_d T}{\pi}. \tag{48}$$

The same definition holds for multilevels with frequency assignments which make the frequency spacing uniform and equal to that for the binary case. The frequencies nearest to the carrier are located at $\omega_c \pm \omega_d$, the intermediate frequencies are at $\omega_c \pm (2n - 1)\omega_d$, and the ones furthest from the carrier are at $\omega_c \pm (N - 1)\omega_d$, where N is the number of levels. Thus, the frequency band of the power spectrum will increase approximately with N for constant k. The frequency band occupied can be kept approximately the same by letting k decrease with N.

In this example, the random variables a_n are discrete and may be represented as

$$a_n = 2n - (N + 1), \qquad n = 1, 2, \cdots, N. \tag{49}$$

The argument of F in (43) is

$$\gamma_n = (\omega - \omega_c - a_n\omega_d)T/2 = (\beta - a_n k/2)\pi, \tag{50}$$

and the equations in (47) become

$$\begin{aligned} I_1 &= \frac{1}{N} \sum_{n=1}^{N} \left[\frac{\sin \gamma_n}{\gamma_n}\right]^2 \\ I_2^2 &= \frac{1}{N^2} \sum_{n=1}^{N} \sum_{m=1}^{N} \exp -i(\gamma_n + \gamma_m) \frac{\sin \gamma_n}{\gamma_n} \frac{\sin \gamma_m}{\gamma_m}. \end{aligned} \tag{51}$$

Since we can alternatively write

$$a_n = \pm(2n - 1), \qquad n = 1, 2, \cdots, N/2$$

we have that

$$\begin{aligned} C_a(\omega_d T) = C_a(k\pi) &= \sum_n P_r(a_n) \exp (i\omega_d a_n T) \\ &= (1/N) \sum_{n=1}^{N/2} [e^{ik\pi(2n-1)} + e^{-ik\pi(2n-1)}] \\ &= (2/N) \sum_{n=1}^{N/2} \cos k\pi(2n - 1). \end{aligned} \tag{52}$$

The complex terms from (46) are

$$\begin{aligned} B &= \mathrm{Re}\left[\frac{e^{-i(\gamma_n+\gamma_m)}}{1 - C_a e^{-2\pi\beta}}\right] \\ &= \frac{\cos (\gamma_n + \gamma_m) - C_a \cos (\gamma_n + \gamma_m - 2\pi\beta)}{1 + C_a^2 - 2C_a \cos 2\pi\beta}. \end{aligned} \tag{53}$$

We can now write the N-level normalized spectral density as

$$\frac{G(\beta)}{A^2T} = \frac{1}{N}\sum_{n=1}^{N}\left[\frac{1}{2}\frac{\sin^2\gamma_n}{\gamma_n^2} + \frac{1}{N}\sum_{m=1}^{N} B\,\frac{\sin\gamma_n}{\gamma_n}\frac{\sin\gamma_m}{\gamma_m}\right], \tag{54}$$

where γ_n and B are given by (50) and (53).

Using several values of the two parameters — N, the number of levels and k, the deviation — we have calculated numerically the spectral densities from the relations given above, and plotted them against the normalized frequency $\beta = (\omega - \omega_c)T/2\pi$. On this scale, ω_d occurs at $k/2$ for all values of N.

A large number of spectra are presented to indicate the way the shape changes as the frequency deviation varies. For binary FM, these are given in Fig. 1. We point out that the spectra for the binary cases

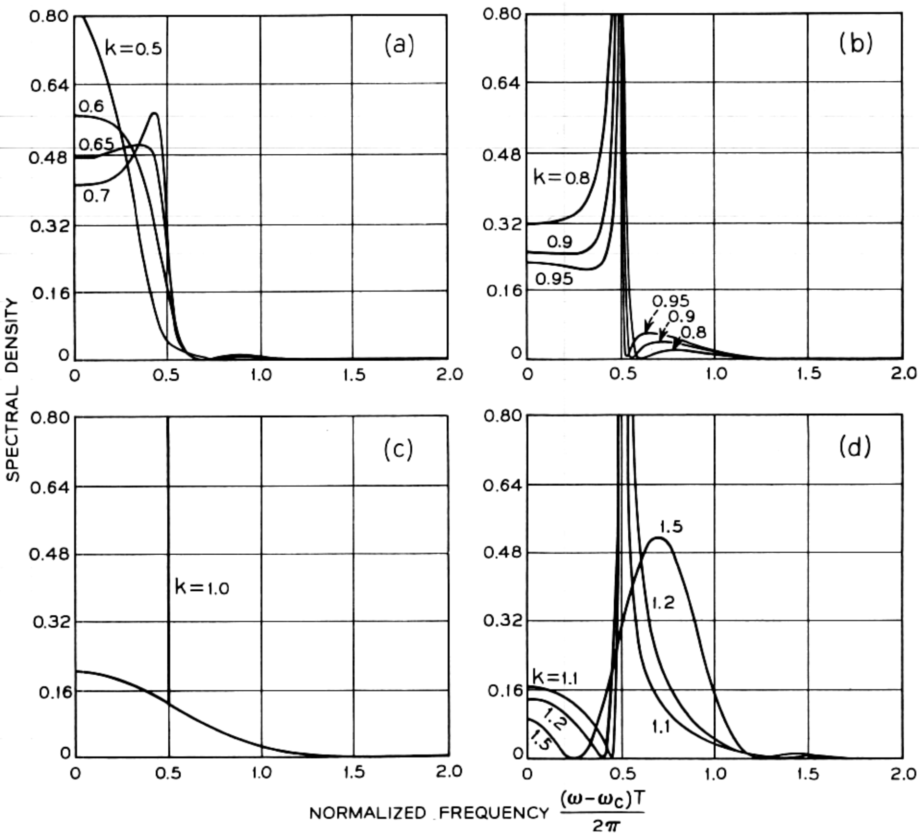

Fig. 1 — Spectral density for 2-level FM.

are the same as those given by Bennett and Rice, *op cit*, except that the origin of the frequency scale has been shifted from the lower (space) frequency to midband.

The spectra for 4- and 8-level FM are given in Figs. 2 and 3, respectively. The multilevel cases show considerable similarity to the binary ones. For small values of k, the spectra are narrow and decrease smoothly towards zero. In particular, Fig. 4 shows the spectra for $k = 1/N$, and these three are nearly identical. As k increases towards unity the spectrum widens, and as predicted, there tends to be concentration of power about the *a priori* chosen frequencies. This concentration is especially marked in the range $1 - 1/2N < k < 1 + 1/2N$. At $k = 1$, there is a spectral line at the frequency $\frac{1}{2}$, and its odd multiples. As k increases from unity the concentration at ω_d is again broadened, and reduced in intensity. We attempt to show these features in several plots as a function of k.

Fig. 5 shows the decrease in spectral density at zero (mid-band) frequency with increasing k. For higher level systems the zero-frequency level is less for any value of k, but the decrease with k is slower.

The position of the spectral peaks, as a function of k for the 8-level system is shown in Fig. 6. Other level systems show similar behavior. For $k = 1$, the *a priori* chosen frequencies are (measured from the carrier) at $\pm(2n - 1)/2$, and the delta functions in the spectral density occur at these same frequencies. For $k < 1$, the peaks of the spectral density are no longer delta functions, and they occur nearer the carrier than the chosen frequencies. They are further from the carrier for $k > 1$.

An interesting phenomenon is observed for the cases where k is the reciprocal of the number of levels. For these relations the principal portion of the spectrum is confined to a relatively narrow band. These curves have approximately the same shape as seen from the curves in Fig. 4 and the following table:

No. of Levels	k	Spectral Density at Freq = 0	.25	.5	.75
2	0.500	0.810	0.500	0.090	0.00
4	0.250	0.750	0.470	0.117	0.011
8	0.125	0.735	0.430	0.124	0.013

The program was extended to calculate the power in the continuous portion of the spectrum. For all values of N, and for k away from unity this power is $\frac{1}{2}$, and for $k = 1$, this power is $\frac{1}{2} - 1/2N$. Thus the total power in the spectral lines is $1/2N$. Clearly the power in each line is $1/2N^2$ since they are assumed to have uniform likelihood of occurrence. It is

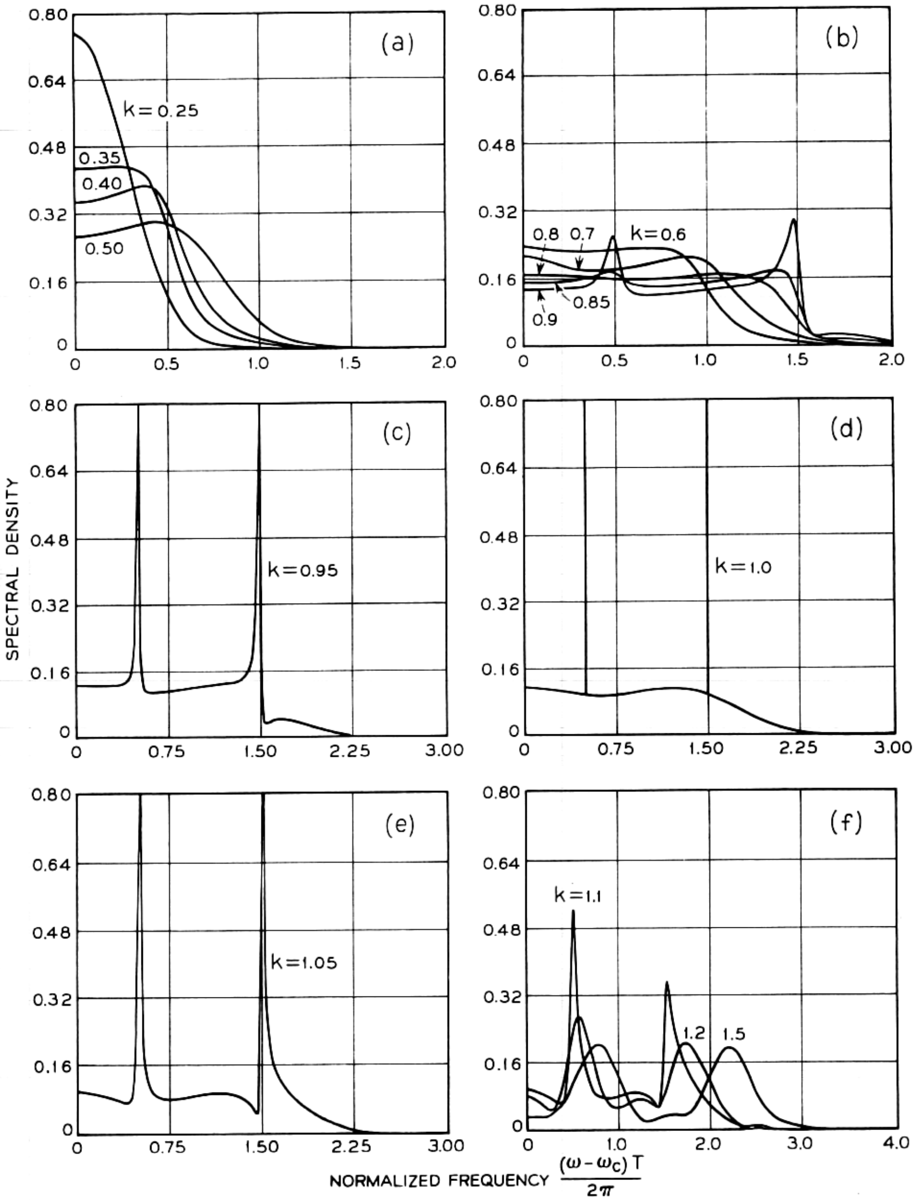

Fig. 2 — Spectral density for 4-level FM.

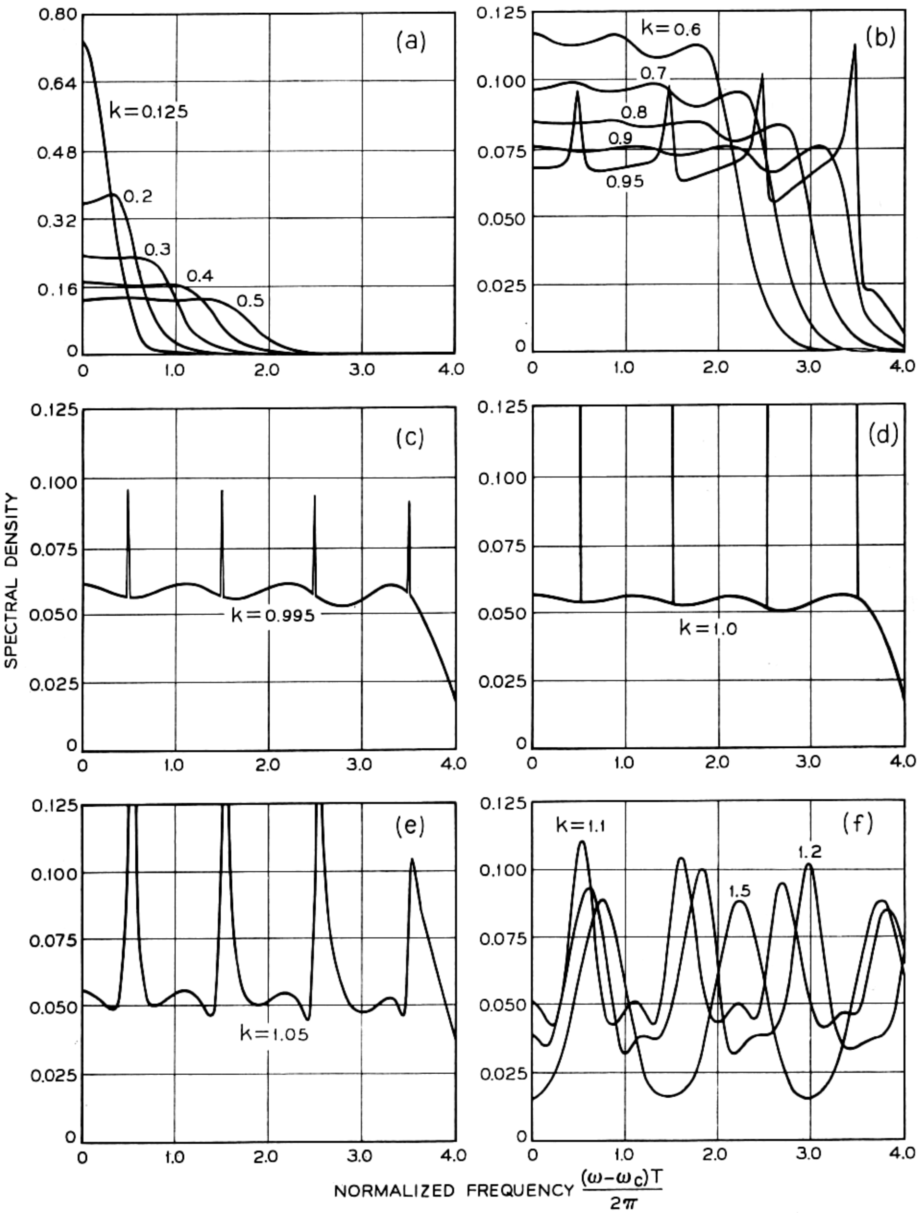

Fig. 3 — Spectral density for 8-level FM.

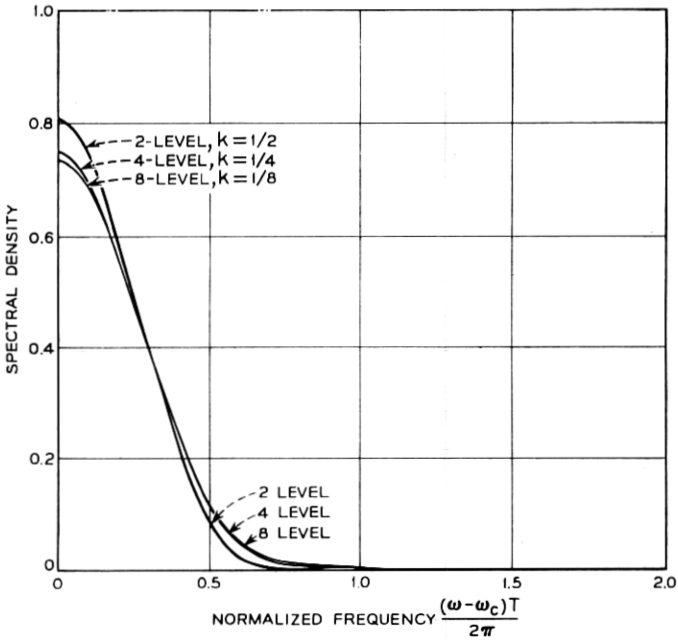

Fig. 4 — Spectral density for $k = 1/\text{No. of levels}$.

also very easy to show from (40) that this is the expected division of power between the continuous spectrum and the discrete spectral lines.

We also thought it interesting to exhibit spectral shapes when the a_n's have a gaussian probability distribution. This situation may arise in pulse frequency modulation with baseband amplitude samples possessing gaussian probability densities. In this case, the probability density of the a_n's is

$$P(a_n) = \frac{1}{\sqrt{2\pi}\,\sigma} \exp\left(-\frac{a_n^2}{2\sigma^2}\right) = \frac{1}{\sqrt{2\pi}\,\sigma} \exp\left[-\frac{(\gamma - \beta\pi)^2}{2\mu^2}\right], \qquad (55)$$

and the characteristic function is

$$C_a(\omega_d T) = \exp\left[-\frac{(\omega_d T\sigma)^2}{2}\right] = \exp\,(-2\mu^2),$$

where

$$\mu = \omega_d T\sigma/2,$$

$$(56)$$

and

$$\gamma = \beta\pi - a\mu/\sigma.$$

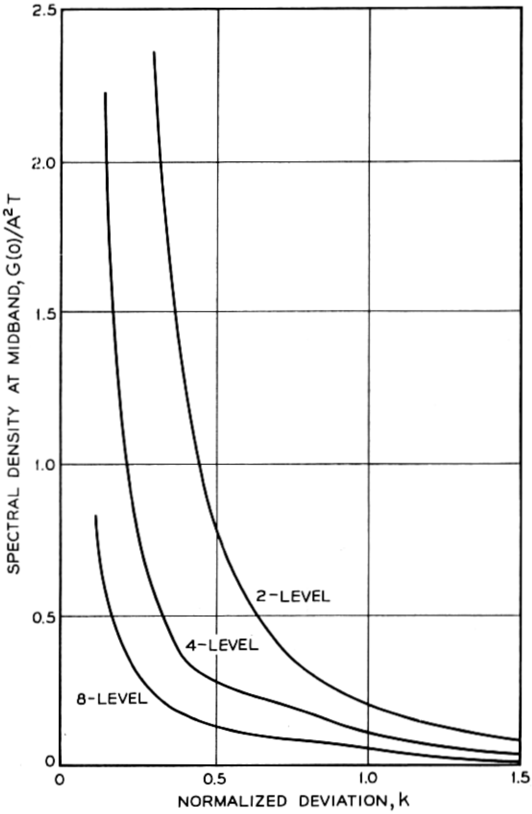

Fig. 5 — Spectral density at midband — Discrete multilevel case.

Equation (51) can be written as

$$I_1 = \frac{1}{\sqrt{2\pi}\,\mu} \int_{-\infty}^{\infty} \frac{\sin^2 \gamma}{\gamma^2} \exp\left[-\frac{(\gamma - \beta\pi)^2}{2\mu^2}\right] d\gamma, \tag{57}$$

$$I_2 = \frac{1}{\sqrt{2\pi}\,\mu} \int_{-\infty}^{\infty} \frac{\sin \gamma}{\gamma}\, e^{-i\gamma} \exp\left[-\frac{(\gamma - \beta\pi)^2}{2\mu^2}\right] d\gamma.$$

Using elementary reductions I_1 is written as

$$I_1 = \frac{\exp\left[-\frac{1}{2}\left(\frac{\beta\pi}{\mu}\right)^2\right]}{2} \int_{-2}^{2} \left(1 - \frac{|z|}{2}\right) \exp\left[-\frac{1}{2}\left(\mu z - i\frac{\beta\pi}{\mu}\right)^2\right] dz. \tag{58}$$

Let

$$t = (xz/2) - iy$$
$$t_1 = iy \qquad (59)$$
$$t_2 = x + iy$$

where

$$x = \sqrt{2}\,\mu, \qquad y = \pi\beta/\sqrt{2}\,\mu. \qquad (60)$$

Then

$$I_1 = \frac{2(Ax - By)}{x^2} + \frac{e^{-x^2}\cos 2\pi\beta - 1}{x^2}, \qquad (61)$$

where

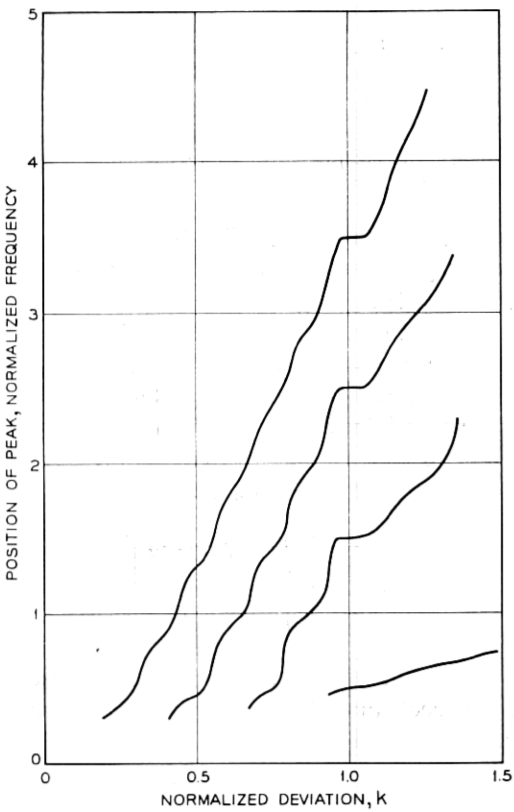

Fig. 6 — Position of spectral peaks — Discrete multilevel case.

$$\begin{aligned} A &= e^{-y^2} \operatorname{Re}\left(\int_0^{t_2} e^{-t^2}\, dt - \int_0^{t_1} e^{-t^2}\, dt\right) \\ B &= e^{-y^2} \operatorname{Im}\left(\int_0^{t_2} e^{-t^2}\, dt - \int_0^{t_1} e^{-t^2}\, dt\right). \end{aligned} \tag{62}$$

In this same manner,

$$\begin{aligned} I_2 &= \frac{1}{2\pi} \int_{-\infty}^{\tau} dz \exp\left(-i\beta\pi z - \frac{\mu^2 z^2}{2}\right) \int_{-\infty}^{\infty} d\gamma \frac{\sin \gamma}{\gamma} e^{-i\gamma_e - i\gamma z} \\ &= \frac{A - iB}{x} \end{aligned} \tag{63}$$

and

$$I_2^2 = \frac{A^2 - B^2 - 2iAB}{x^2}. \tag{64}$$

Substituting (61) and (64) into (46) we obtain

$$\begin{aligned} \frac{G(\beta)}{A^2T} = \frac{1}{2x^2}\Bigg[& 2(Ax - \beta y) + e^{-x^2} \cos 2\pi\beta - 1 \\ & + \frac{(A^2 - B^2)(e^{-x^2} - \cos 2\pi\beta) + 2AB \cos 2\pi\beta}{\cosh x^2 - \cos 2\pi\beta}\Bigg]. \end{aligned} \tag{65}$$

In this case the deviation is controlled by the parameter $\mu = \omega_d T\sigma/2$. In Fig. 7 we display the spectra for several values of this parameter. When $\mu = 0$, the spectrum is a delta function at $\beta = 0$ (midband). As μ increases the spectrum widens, approximately as μ and the midband value decreases approximately as μ^{-2}, for small μ, and as μ^{-1} for larger values. We show these two trends in Figs. 8 and 9.

The values of spectral density at $\beta = 0$, together with the asymptotes, are shown in Fig. 8. Two estimates of the width are shown in Fig. 9. From the definition of the Gabor bandwidth, Ref. 7,

$$\sigma_G = \left[\frac{\int_0^{\infty} G(\beta)\beta^2 d\beta}{\int_0^{\infty} G(\beta)\, d\beta}\right]^{\frac{1}{2}}. \tag{66}$$

We note that σ_G is very nearly equal to μ/π. That is, the standard deviation of the power spectrum is the same as the standard deviation of the input times the normalized deviation frequency:

$$\sigma_G \doteqdot \sigma\ (\omega_d T/2\pi). \tag{67}$$

Another estimate of the width of the power spectrum comes from the value of β at which the density has fallen by e, namely

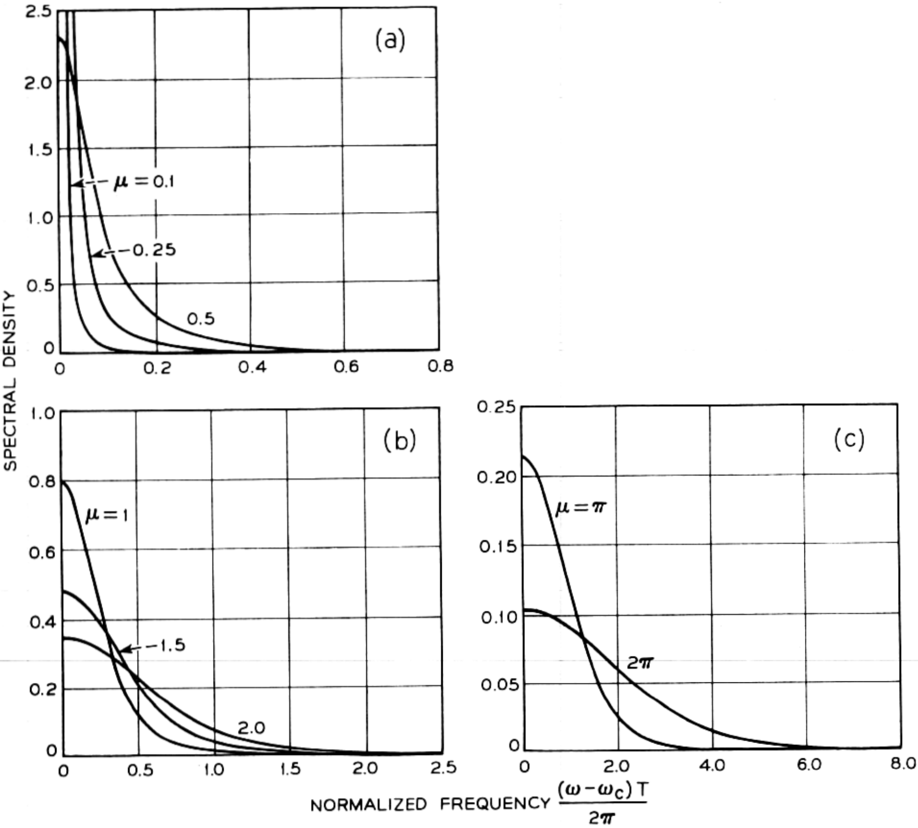

Fig. 7 — Spectral density for gaussian distribution.

$$\sigma_E = \frac{\beta}{\sqrt{\pi}} \quad \text{at} \quad \frac{G(0)}{e}. \tag{68}$$

At high values of σ, where the spectral density curves appear more nearly gaussian, σ_E approaches σ_G.

The gaussian case spectral density curves were also integrated to obtain the power. We obtain $\frac{1}{2}$ in all cases, thus providing a check on our work. It is interesting to note that even for μ as low as 0.5, 98 per cent of the power lies within $3\sigma_G$ of midband.

V. SUMMARY OF CURVES

Spectra are presented for 2, 4, and 8 equally-spaced uniformly distributed frequencies and for normally distributed frequencies. The gen-

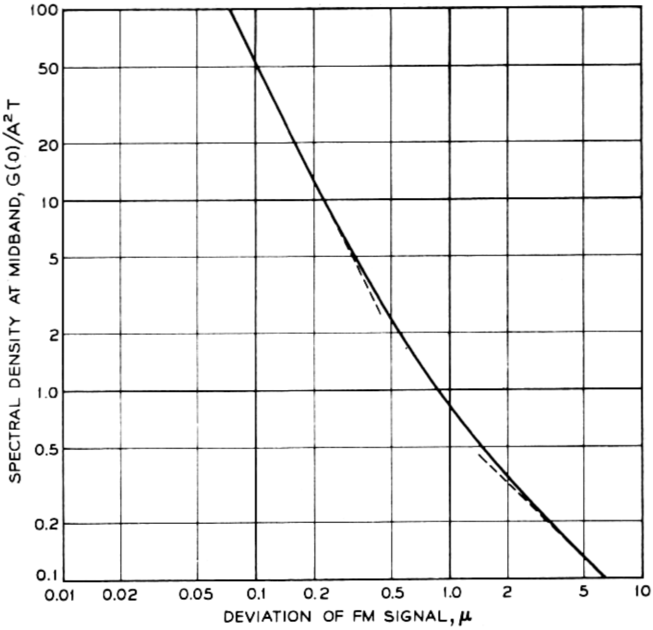

Fig. 8 — Spectral density at midband — Gaussian case.

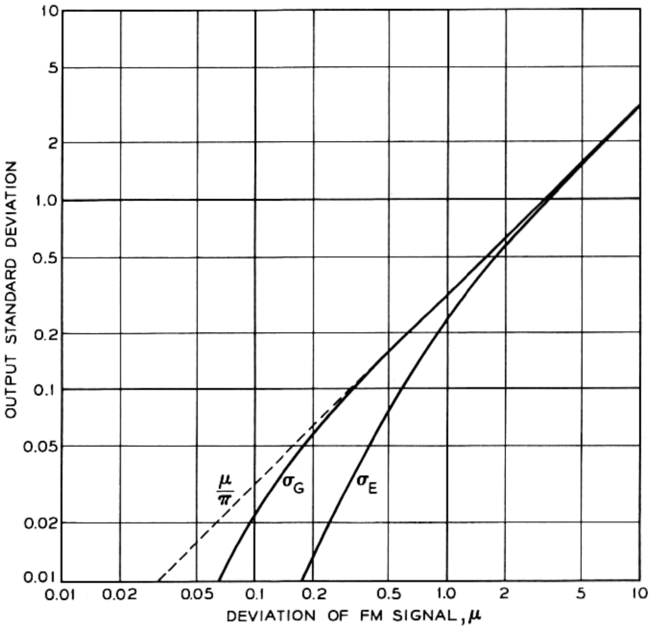

Fig. 9 — Standard deviation of spectral density function — Gaussian case.

eral trend of the curves, as a function of the frequency deviation, is shown in Figs. 5, 6, 8, and 9. As expected, the band occupied by a significant portion of the spectrum increases with the deviation.

For the discrete multilevel case, the frequency deviation parameter is $k = \omega_d T/\pi$. For $k = 1/N$ the spectral density functions for different N are nearly identical. They are relatively narrow and decrease smoothly to zero. Line spectra occur at the *a priori* chosen frequencies when k is an integer.

For the gaussian case the deviation parameter is $\mu = \sigma\omega_d T/2$. For large μ, the shape of the spectral density approaches a gaussian curve with a standard deviation of $\sigma\omega_d T/2\pi$. For lower μ, the curves are slightly narrower with correspondingly longer tails. The maximum value for each μ, which occurs at $\beta = 0$, approaches $\frac{1}{2}\mu^2$ for small μ and $2/\pi\mu$ for large values.

REFERENCES

1. Salz, J., Performance of Multilevel Narrow-Band FM Digital Communication Systems, to be published.
2. Bennett, W. R., and Rice, S. O., Spectral Density and Autocorrelation Functions Associated with Binary Frequency Shift Keying, B.S.T.J., *42*, Sept. 1963.
3. Salz, J., Spectral Density Function of Multilevel Continuous Phase FM, IEEE Trans. Information Theory, July, 1965.
4. Loève, M., *Probability Theory*, D. Van Nostrand Company, pp. 201–202, 1960.
5. Lighthill, M. J., *An Introduction to Fourier Analysis and Generalized Functions*, Cambridge University Press, 1959.
6. Barnard, R. D., A Note on a Special Class of One-Sided Distribution Sums, B.S.T.J., *44*, Nov., 1965.
7. Gabor, D., Theory of Communication, J. Inst. Elect. Engrs., *93* III, p. 429.